Int. J. Electrochem. Sci., 16 **(2021)** Article ID: 210252, doi: 10.20964/2021.02.03

International Journal of ELECTROCHEMICAL SCIENCE
www.electrochemsci.org

Short Communication

Electrochemical Study on Stability and Corrosion Resistance of low-alloy En39B Reinforcing steel Bar Embedded in Concrete Immersed in Soil Containing Chloride Ions

Jingying Song[*], *Hualei Li, Hongwei Feng*

School of Civil Engineering and Architecture, Xinxiang University, Xinxiang, 453003, Henan, China
[*]E-mail: ss37843011@163.com

Received: 31 October 2020 / *Accepted:* 25 November 2020 / *Published:* 31 December 2020

In this work, an electrochemical study on stability and corrosion resistance of low-alloy En39B reinforcing steel bars embedded in concrete immersed to soil contaminated with chloride was performed. The corrosion behavior of En39B steel rebar was studied by electrochemical impedance spectroscopy and polarization analysis. Electrochemical results revealed that the high content of Cr in steel rebar had a significant improvement in the polarization resistance value, showing a high corrosion resistance for En39B sample. The mass-loss measurements revealed a reduction of mass-loss rate in En39B steel rebar due to the higher content of Cr compared to the EN36A which was completely consistent with the results from EIS analysis. The potentiodynamic polarization results indicate that the performance of corrosion resistant in En39B steel reinforced concrete considerably improved with formation of a passive layer to restrain both the anodic and the cathodic corrosion reaction. The surface morphology of En39B immersed in soil contaminated with 3.5 wt% NaCl revealed the formation of low corrosion products on steel which was in agreement with the results achieved from electrochemical assessments.

Keywords: Corrosion resistance; Electrochemical study; Reinforced concrete; low-alloy steel rebar; Soil contaminated with chloride

1. INTRODUCTION

Chloride (Cl) ions are the major cause of corrosion in reinforced concrete structures, the Cl^- ions can be present in concrete mixture components such as additives, cement, water, aggregates, or through the environment with which reinforced concrete structure is in contact, for example industrial water, sewage water, sea water and contaminated soils [1, 2]. The Cl^- ions are capable of producing localized corrosion of steel rebar and hence to produce the unexpected and premature failure of the structures [3, 4]. Corrosion of steel reinforced concrete structures is known as a problem of social importance and great economic, in the past decades, it has worked hard to reduce the consequences of this phenomenon [5, 6].

There are numerous works around the world that face the problem from various perspectives, from innovation in cement and concrete technology as lightweight concrete structure reinforced by synthetic or steel fibers, corrosion inhibitors and assessment of corrosion concrete immersed in different corrosive environments [7, 8]. Recent studies exhibited that micro-alloyed steel rebar may be considered in aggressive environments. By addition of anti-corrosion alloy elements, like aluminum, chromium, molybdenum, nickel, silicon and copper, the corrosion resistance of steel reinforcement can be improved compared to the common carbon steel rebar [9, 10]. Though, because of the low amount of alloy elements used, the production costs can be significantly reduced. Thus, this alloyed steel rebar has great potential which can be utilized as a replacement bar for the carbon steel rebar with much longer durability in a corrosive environment [11, 12].

The present work was performed to evaluate the electrochemical behavior of steel reinforced concrete structures buried into a soil contaminated with Cl ions which are able to attain parameters which allow us to evaluate the corrosive behavior of the subsoil, to make more durable structures and corrosion resistant. Moreover, much research has focused on the effect of alloying elements on the corrosion of steel reinforced concrete in an aggressive environment. However, the studies in chromium (Cr) content on carbon steel rebar by electrochemical procedure have not been yet published. Hence, in this research, the effect of Cr content on electrochemical corrosion behavior of steel rebar immersed to soil contaminated with chloride were investigated.

2. MATERIALS AND METHOD

In this work, cylinders of Portland cement (PC) reinforced with EN39B and EN36A steel rebar with diameter of 6 mm and height of 10 cm were used to evaluate the corrosion resistance of alloyed steel bar in soil environment contaminated with chloride. The PC was blended with sand, gravel, and water (1.5: 3: 1: 0.5) to produce concrete structure. The components of cement were mixed via a high-speed mixer machine for obtaining a heterogeneous dispersion. Alloyed steel rebars were applied as working electrodes in the electrochemical process. The chemical composition of alloyed steel bars are presented in table 1.

In order to determine the corrosion of alloyed steel reinforced concrete samples, these samples were buried into a soil type silt of higher plastic (MH) contaminated with 3.5 wt% NaCl as aggressive agent by weight of soil.

Table 1. Chemical composition of alloyed steel rebar (wt%)

Alloys	C	Mn	Si	Ni	Cr	Fe
EN39B	0.12	0.35	0.15	3.9	1.4	Residual
EN36A	0.12	0.35	0.15	3.75	0.72	Residual

A three-electrode cell was used during the electrochemical tests, with EN39B steel and saturated calomel and platinum electrodes as a working, reference, and counter electrodes, respectively. Electrochemical impedance spectroscopy (EIS) analysis was performed at the frequency wide-ranging between 0.1 MHz and 10 mHz at 10 mV applied AC amplitude. The cyclic voltammetry (CV) analysis was done between -1.5V and 1.5 V at scan rate with 20 mV/s. Evaluations were periodically performed after 1, 2, 3 and 4 months of exposure. The potentiodynamic polarization characterizations were done at a scanning rate of 1 mV/s. The surface morphologies of the steel samples were conducted using scanning electron microscope (SEM).

The weight loss technique was performed according to the ASTM standards using different samples. These samples were also cleaned by 600 grit silicon carbide papers, rinsed with distilled water, degreased with acetone and dried under a warm air stream. Before the immersion, the specimens were weighted in an analytical balance Adventurer Ohaus model AR2114 with a precision of 0.0001g. After the immersion time, the samples were cleaned from the corrosion products, and then weighted again in the same analytical balance. The difference between the initial and final weights divided between the initial areas was the mass loss.

3. RESULTS AND DISCUSSION

To evaluate the formation of passive film and redox reactions on the specimens in the soil environment, CV method was used. Figure 1 indicates the CV curves of the specimens in the soil contaminated with 3.5 wt% NaCl. The cathodic and anodic peak potentials were found as revealed in Fig. 1.

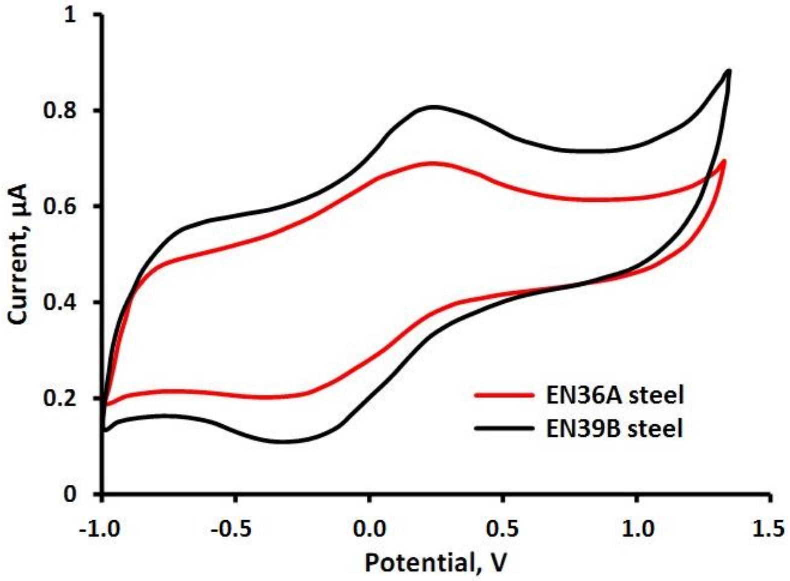

Figure 1. CV of the different steel reinforced concrete exposed to the soil contaminated with 3.5 wt% NaCl.

The anodic peak seemed at about potential of 0.15 V for both samples that is attributed to the reactions 1-3. It approves the transformation of Fe^{2+} to Fe^{3+} ion and the formation of passive film on the steel surface [13]:

$$Fe+2OH^{-} \leftrightarrow Fe(OH)2 +2e^{-} \quad (1)$$

$$3Fe(OH)_2 + 2OH^{-} \leftrightarrow Fe_3O_4 + 4H_2O + 2e^{-} \quad (2)$$

$$3FeO+ 2OH^{-} \leftrightarrow Fe_3O_4+ 2e^{-} \quad (3)$$

As earlier reported, the current-density in zero-potential (i_0) can show the corrosion resistance of passive film [14]: the higher i_0 suggests weaker corrosion resistance. When Cr content increases, i_0 reduces. This reduction indicates that small amount of Cr micro-alloy in steel reinforcement helps the stability of passive layer formation. As the potential rises up to 0.8 V, the anodic current-density rapidly increases which may be related to the electrochemical procedure controlled by evolution of O_2 molecule. As shown in Fig. 1, the cathodic peak observed at potential of -0.26V. When the potential shifts toward more negative values, the cathodic current-density increases quickly which may be related to the electrochemical procedure controlled by evolution of H_2 molecule. Moreover, the anodic peak of EN39B bar is lower than the EN36A sample. Thus, the increase in Cr content in steel bar can improve passive layer stability and corrosion resistance.

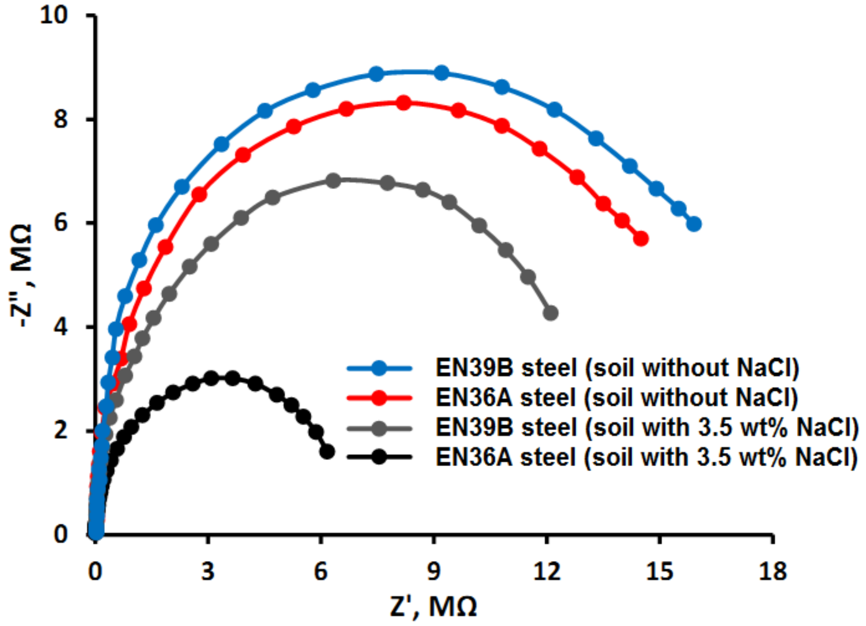

Figure 2. EIS of the specimens with different Cr content exposed to soil contaminated with and without 3.5 wt% NaCl.

EIS method has been widely used in the study of the passive layer on steel surface because of its capability to analyze redox reactions of the steel bars in a salty environment [15]. EIS was done to characterize the effect of Cr micro-alloy onto the corrosion behavior of steel bars with passive films in soil contaminated with and without 3.5 wt% NaCl. Figure 3 shows an equivalent circuit model which proposed to simulate the electrochemical process. R_m indicates the resistance of mortar which related to the high-frequency response [16]. Given that the electrolyte resistance was insignificant in comparison of the mortar resistance in this work, then the electrolyte resistance was ignored.

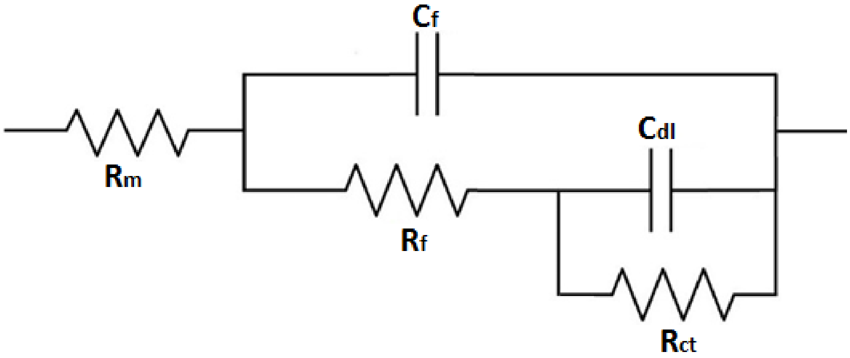

Figure 3. Used equivalent circuit model

During the passivity procedure, the parameters of second-time constant found at the low-frequencies such as C_{dl} and R_{ct} were attributed to the non-ideal interfacial capacitance and charge-transfer resistance of the alloy steel surface. It revealed that the corrosion resistance of the steel bar was controlled through the passive layer properties [17, 18]. The parameters of first-time constant found at the low-frequencies such as C_f and R_f and were recognized to the redox-transformation in corrosion products which occurred on the surface of oxide film.

Polarization resistance (R_p) is an assessable indicator to study the resistance of steel corrosion into the aggressive environment. The higher value of R_p reveals higher corrosion resistance of steel bars.

Furthermore, figure 2 indicates the Nyquist diagrams of carbon steel reinforced concrete exposed to soil contaminated with and without 3.5 wt% NaCl revealed a capacitive arc at low frequency. The capacitive arc radius decreases in soil contaminated with 3.5 wt% NaCl. The semi-circular arc radius in the EIS measurement is related to the polarization resistance of the passive film (table 2). A reduction in the overall impedance values in soil contaminated with 3.5 wt% NaCl reveals a decrease of the corrosion resistance which is in good accordance with the previous studies.

Table 2. Electrochemical parameters obtained from the EIS analysis

Steel	Soil	R_m (Ω cm^2)	R_f(MΩ cm^2)	C_f(μF cm^{-2})	R_{ct} (MΩ cm^2)	C_{dl}(μF cm^{-2})	R_p (MΩ cm^2)
EN36A	with 3.5 wt% NaCl	58.2	4.36	2.7	7.22	3.4	11.58
	without NaCl	47.9	14.74	1.2	18.96	1.7	33.70
EN39B	with 3.5 wt% NaCl	62.4	7.83	1.9	13.57	2.5	21.40
	without NaCl	53.6	16.58	0.8	21.75	1.3	38.33

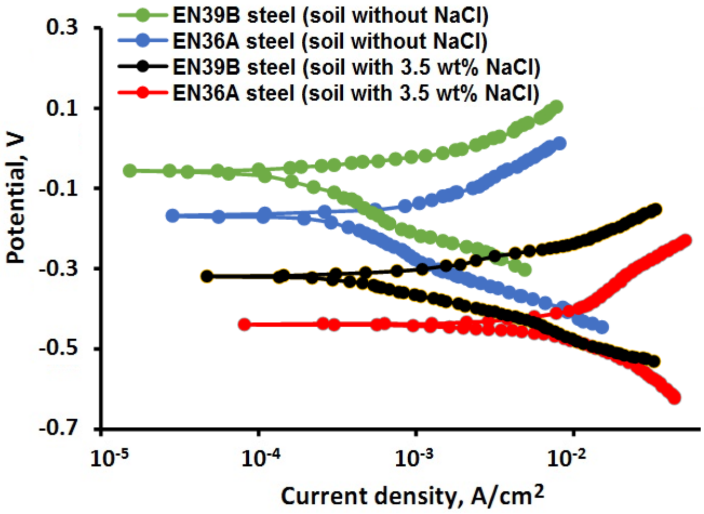

Figure 4. Polarization Plots of alloy steel rebars in soil contaminated with and without 3.5 wt% NaCl

According to table 2, increasing the Cr contents exhibit a significant improvement in R_p value demonstrating higher corrosion resistance for EN39B steel rebar.

The corrosion resistance of samples can be considered by the polarization analysis. Hence, a polarization assessment was done to study the electrochemical process of alloy steels. Figure 4 exhibits the polarization curves of the samples in soil contaminated with and without 3.5 wt% NaCl. Commonly, both steel samples indicate no active corrosion and passivation behavior, revealing the anodic current density improved continuously by increasing potential. In this study, the corrosion potential was moved toward more noble direction and current-density at the anode reduced slightly due to the increase of Cr element, showing the improved corrosion resistance by the increasing Cr in alloy. The corrosion rates were calculated by the Tafel extrapolation method. As stated by Faraday's law, corrosion rate may be determined by the corrosion current-density [19]:

$$Corrosion\ rate\left(\frac{mm}{y}\right) = \frac{3.16\times10^{8} i_{corr} M}{zF_{\rho}} \quad (1)$$

where i_{corr} and M indicate the corrosion current-density and the molar mass, respectively. z and F represent the number of electrons transferred in a metal atom and Faraday's constant, respectively. ρ reveals the metal density (g/cm^3).

The corrosion potential of EN39B was considerably more positive than the EN36A steel rebar, which shows that the self-corrosion potential improved after the increase of Cr. Moreover, the cathodic curves of EN39B shifted downwards with increasing Cr content, indicating the cathode reaction rates were comparatively lower at this phase [15]. The polarization data are shown in table 3 which indicates the appreciated effects of Cr alloy. The changes in the corrosion rates may be because of the ohmic drop produced by the resistance of solution, which happened during the polarization assessment [16].

Table 3. Fitting parameters of the specimens achieved from polarization plots

Steel	Soil	Corrosion potential (mV)	Corrosion current density (mAcm^{-2})	Corrosion rate (mm/year)
EN36A	with 3.5 wt% NaCl	-445	7.63	5.6
	without NaCl	-162	0.74	2.3
EN39B	with 3.5 wt% NaCl	-321	0.86	2.4
	without NaCl	-96	0.47	1.7

As revealed in table 3, the corrosion rate reduction in EN39B can be related to the amount of Cr in alloyed steel bars, which causes more resistance to the steel corrosion in reinforced concrete.

Furthermore, figure 4 shows the results obtained from the reinforced concrete specimens buried to a fine soil type MH, in the natural state without addition of NaCl. It is perfectly observed the difference between the two types of steel used as reinforcement. Both steels have a tendency from the curing stage to more positive value of potential. Also, the investigation of all the obtained results from polarization tests confirmed the influence and aggressiveness of the marine environment soil in comparison to the soil type MH, without any addition of NaCl, soil in its natural state.

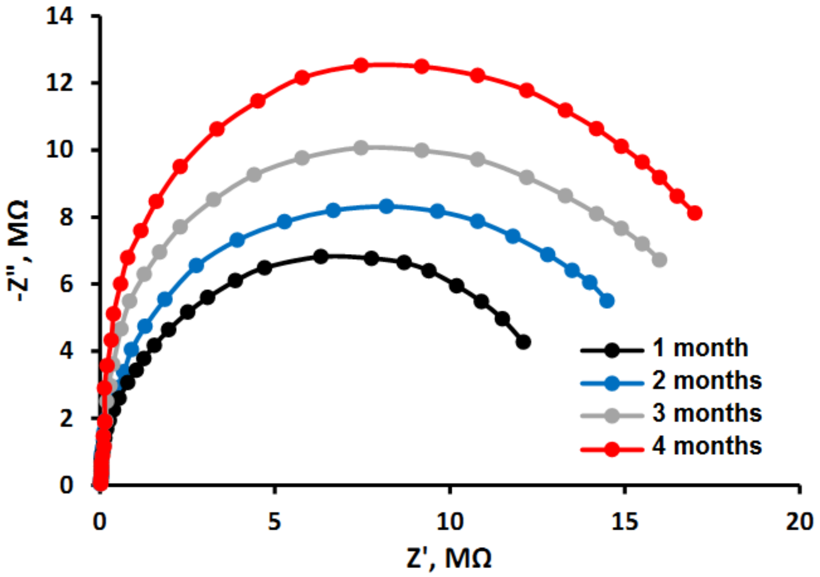

Figure 5. EIS diagrams of the low-alloy En39B reinforcing steel bar embedded in concrete exposed into soil contaminated with 3.5 wt% NaCl at different exposure times

Table 4. Electrochemical parameters from the fitting the equivalent circuit

Exposure time (month)	**R_m (Ω)**	**R_f (MΩ)**	**C_f (μF cm^{-2})**	**R_{ct} (MΩ)**	**C_{dl} (μF cm^{-2})**
1	62.4	7.83	1.9	13.57	2.5
2	54.5	12.51	1.8	17.82	2.3
3	55.8	14.12	1.7	19.75	2.1
4	57.5	16.74	1.6	22.43	1.8

Figure 5 shows Nyquist plots of the samples exposed into soil contaminated with 3.5 wt% NaCl at different exposure times. The best fitting elements based on the electrical circuit revealed in figure 4 are listed in Table 4. Results indicate that the R_{ct} increased about two times from 1 to 4 months exposure time, with a reduction in the C_{dl} from 2.5 to 1.8 μF cm^{-2}, possibly due to hydration products having a higher density and the efficiently refined the pore structure of the reinforced concretes in 4 months exposure time. Bragança et al. [20] reported comparable behavior, with a reduction in capacitance. Furthermore, the corrosion resistance of the steel rebar enhanced after 4 months compared to one month exposure time which can be attributed to the pore size refinement, tortuosity and distribution of capillary pores and also chemical interactions between cement compounds and adsorbed ions [21]. Moreover, The C_f remained stable for all exposure time, demonstrating no degradation in the protective oxide layer on the steel rebar, as expected for an immersion time limit.

Mass-loss and mass-loss rate for alloy steel bars during four weeks exposure time are shown in Fig. 5. Clearly, continuing corrosion attack reasons increased mass-loss, and the average mass-loss rate of the EN39B specimen in each interval was lower than the EN36A specimen. As shown in Fig. 5b, the mass-loss rate of both samples reduced rapidly during the initial one-week and had a slower reduction in the mass-loss rate during long period corrosion. According to previous studies, the reduction in mass-loss rate for EN39B steel rebar can be associated with the mechanical isolation effect of the corrosion film onto direct contact between the bar matrix and the salt mist [22, 23]. Furthermore, the EN39B bar revealed a comparatively lower mass-loss rate during the assessment.

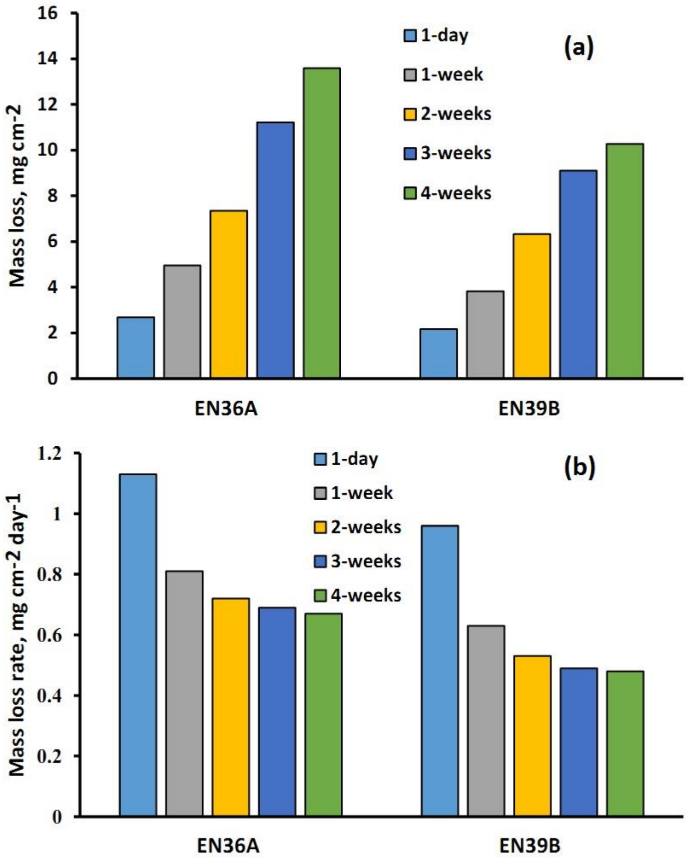

Figure 5. (a) Mass loss and (b) Mass loss rate of the alloy steel bars with different Cr content during 4-weeks of immersion time in soil contaminated with 3.5 wt% NaCl

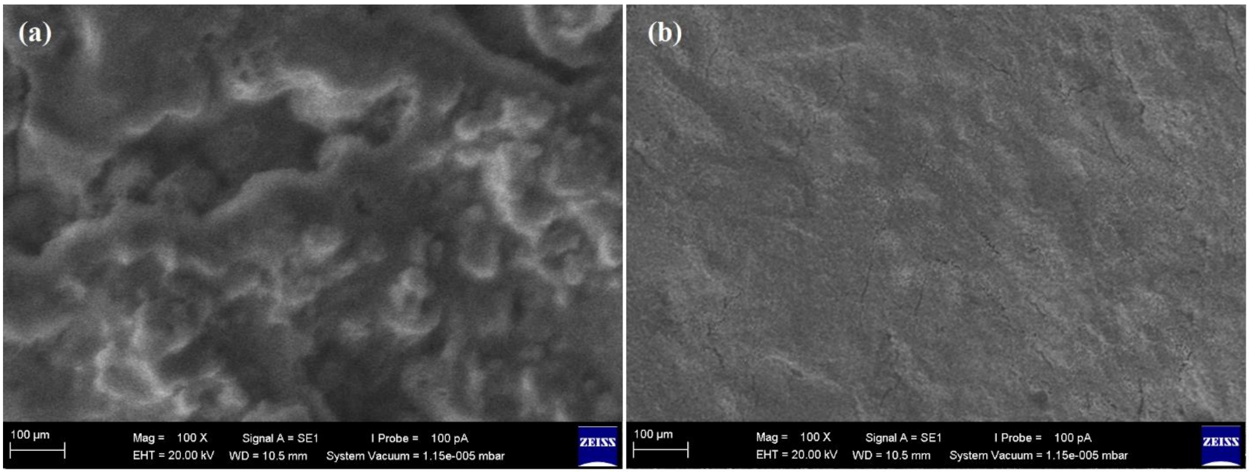

Figure 6. FESEM images of (a) EN36A and (b) EN39B steel rebars in soil contaminated with 3.5 wt% NaCl after 4-weeks immersion time

Average rate in initial mass-loss for the EN39B rebar was 0.96 mgcm^{-2}day^{-1}, which was about 15% less than that of EN36A rebar. Additionally, the average rate of mass-loss for the EN39B sample obtained after electrochemical corrosion of four weeks was 0.48 mgcm^{-2}day^{-1}, which was approximately 29.8% less than that of EN36A steel. The lower mass-loss rate for the EN39B in the initial corrosion may enhance the corrosion resistance of the alloy steel matrix before formation of a thick rust layer on the surface of the sample. Besides, in a long-term period of corrosion, since the thick rust layers covered the steel surface, the effect of positive separation can be more important to retard the corrosive medium diffusion. Therefore, the lower mass-loss rate for the EN39B sample can be related to its rust layer.

Figure 6 indicates the FESEM images of alloy steel rebars exposed to the soil contaminated with 3.5 wt% NaCl after 4-weeks immersion time. The corrosion pitting onto the surface of EN36A steel was more severe than the EN39B rebar, signifying that the EN39B revealed a good corrosion resistance.

4. CONCLUSIONS

Recent studies exhibit that the alloyed steel bars can improve the corrosion resistance of steel reinforced concretes exposed to a corrosive environment. In this work, an electrochemical study on stability and corrosion resistance of low-alloy En39B reinforcing steel Bar embedded in Concrete immersed to soil contaminated with chloride was performed. The corrosion behavior of En39B steel rebar was studied by electrochemical impedance spectroscopy and polarization analysis. Electrochemical results revealed that the high content of Cr in steel rebar had a significant improvement in the polarization resistance value, showing a high corrosion resistance for En39B sample. The potentiodynamic polarization results indicate that the performance of corrosion resistant in En39B steel reinforced concrete considerably improved with formation of a passive layer to restrain both the anodic and the cathodic corrosion reaction. The mass-loss measurements revealed a reduction of mass-loss rate in En39B steel rebar due to the higher content of Cr compared to the EN36A which was completely consistent with the results from EIS analysis. The surface morphology of En39B immersed in soil contaminated with 3.5 wt% NaCl revealed the formation of low corrosion products on steel which was in agreement with the results achieved from electrochemical assessments.

References

1. Y. Wang, S. Zhang, D. Niu, L. Su and D. Luo, *Construction and Building Materials*, 234 (2020) 117390.
2. Y. Song, G. Jiang, Y. Chen, P. Zhao and Y. Tian, *Scientific reports*, 7 (2017) 1.
3. R. Jafari and E. Sadeghi, *Corrosion Science*, 160 (2019) 108066.
4. S. Kakooei, H.M. Akil, A. Dolati and J. Rouhi, *Construction and Building Materials*, 35 (2012) 564.
5. M. Alexander and H. Beushausen, *Cement and Concrete Research*, 122 (2019) 17.
6. U.M. Angst, *Corrosion*, 75 (2019) 1420.
7. M.A. Baltazar-Zamora, J.M. Mendoza-Rangel, R. Croche, C. Gaona, C. Hernández, L. López, F. Olguín and F. Almeraya-Calderón, *Frontiers in Materials*, 6 (2019) 257.
8. E. Ariyachandra, S. Peethamparan, S. Patel and A. Orlov, *Cement and Concrete Research*, 137 (2020) 106210.
9. H. Zhou, Y. Wang and T. Ma, *International Journal of Electrochemical Science*, 15 (2020) 3003.
10. S. Li, G. Song, Q. Fu and C. Pan, *Journal of Alloys and Compounds*, 777 (2019) 877.
11. Y. Tian, M. Liu, X. Cheng, C. Dong, G. Wang and X. Li, *Cement and Concrete Composites*, 97 (2019) 190.
12. S. Kakooei, H.M. Akil, M. Jamshidi and J. Rouhi, *Construction and Building Materials*, 27 (2012) 73.
13. E. Volpi, A. Olietti, M. Stefanoni and S.P. Trasatti, *Journal of Electroanalytical Chemistry*, 736 (2015) 38.
14. C. Wang, S. Yang, Y. Chen, B. Wang, J. He and C. Tang, *RSC Advances*, 5 (2015) 34580.
15. L. Yang, G. Yi, Y. Hou, H. Cheng, X. Luo, S.G. Pavlostathis, S. Luo and A. Wang, *Biosensors and Bioelectronics*, 141 (2019) 111444.
16. N. Naderi, M. Hashim and J. Rouhi, *International Journal of Electrochemical Science*, 7 (2012) 8481.
17. H.-S. Ryu, J.K. Singh, H.-S. Lee, M.A. Ismail and W.-J. Park, *Construction and Building Materials*, 133 (2017) 387.
18. M. Husairi, J. Rouhi, K. Alvin, Z. Atikah, M. Rusop and S. Abdullah, *Semiconductor Science and Technology*, 29 (2014) 075015.
19. A.D. King, N. Birbilis and J.R. Scully, *Electrochimica Acta*, 121 (2014) 394.
20. M.O. Bragança, K.F. Portella, M.M. Bonato and C.E. Marino, *Construction and Building Materials*, 68 (2014) 650.
21. P. Gu, P. Xie, J.J. Beaudoin and R. Brousseau, *Cement and Concrete Research*, 23 (1993) 157.
22. H. Tamura, *Corrosion Science*, 50 (2008) 1872.
23. R.E. Melchers, *Corrosion Science*, 68 (2013) 186.